PHYSICAL REVIEW D **91,** 075005 (2015)

Natural SUSY with a bino- or wino-like LSP

Howard Baer,[1,2,*] Vernon Barger,[3,†] Peisi Huang,[4,5,‡] Dan Mickelson,[1,§] Maren Padeffke-Kirkland,[1,‖] and Xerxes Tata[6,¶]

[1]*Dept. of Physics and Astronomy, University of Oklahoma, Norman, Oklahoma 73019, USA*
[2]*William I. Fine Theoretical Physics Institute, University of Minnesota, Minneapolis, Minnesota 55455, USA*
[3]*Dept. of Physics, University of Wisconsin, Madison, Wisconsin 53706, USA*
[4]*HEP Division, Argonne National Lab, Argonne, Illinois 60439, USA*
[5]*Enrico Fermi Institute, University of Chicago, Chicago, Illinois 60637, USA*
[6]*Dept. of Physics and Astronomy, University of Hawaii, Honolulu, Hawaii 96822, USA*

(Received 2 February 2015; published 8 April 2015)

In natural supersymmetry models, Higgsinos are always light because μ^2 cannot be much larger than M_Z^2, while squarks and gluinos may be very heavy. Unless gluinos are discovered at LHC13, the commonly assumed unification of gaugino mass parameters will imply correspondingly heavy winos and binos, resulting in a Higgsino-like lightest supersymmetric particle (LSP) and small inter-Higgsino mass splittings. The small visible energy release in Higgsino decays makes their pair production difficult to detect at the LHC. Relaxing gaugino mass universality allows for relatively light winos and binos without violating LHC gluino mass bounds and without affecting naturalness. In the case where the bino mass $M_1 \lesssim \mu$, then one obtains a mixed bino-Higgsino LSP with instead sizable $\tilde{W}_1 - \tilde{Z}_1$ and $\tilde{Z}_2 - \tilde{Z}_1$ mass gaps. The thermal neutralino abundance can match the measured dark matter density in contrast to models with a Higgsino-like LSP where weakly interacting massive particles are underproduced by factors of 10–15. If instead $M_2 \lesssim \mu$, then one obtains a mixed wino-Higgsino LSP with large $\tilde{Z}_2 - \tilde{Z}_1$ but small $\tilde{W}_1 - \tilde{Z}_1$ mass gaps with still an underabundance of thermally produced weakly interacting massive particles. We discuss dark matter detection in other direct and indirect detection experiments and caution that the bounds from these must be interpreted with care. Finally, we show that LHC13 experiments should be able to probe these nonuniversal mass scenarios via a variety of channels including multilepton + $E_T^{\rm miss}$ events, $WZ + E_T^{\rm miss}$ events, $Wh + E_T^{\rm miss}$ events, and $W^{\pm}W^{\pm} + E_T^{\rm miss}$ events from electroweak chargino and neutralino production.

DOI: 10.1103/PhysRevD.91.075005 PACS numbers: 12.60.Jv, 14.80.Ly, 14.80.Nb

I. INTRODUCTION

Results from the first extended runs of the LHC at $\sqrt{s} = 7$ and 8 TeV have led some authors to imply that there is a crisis in supersymmetry (SUSY) phenomenology [1]: how can it be that the Higgs and vector boson masses—the values of which are related to weak scale soft SUSY breaking (SSB) parameters and to the superpotential parameter μ—are clustered near 100 GeV while superpartner masses—the values of which are also determined by soft SUSY breaking terms—are so heavy that they are beyond the reach of LHC? The superpotential Higgsino mass parameter μ and the SSB Higgs mass parameters enter via the tree-level Higgs potential, whereas other SSB parameters—specifically, those that affect sparticles with the largest couplings to the Higgs sector—only enter at higher order. This is clearly evident, for example, in the well-known expression

$$\frac{M_Z^2}{2} = \frac{m_{H_d}^2 + \Sigma_d^d - (m_{H_u}^2 + \Sigma_u^u)\tan^2\beta}{\tan^2\beta - 1} - \mu^2, \qquad (1)$$

for the Z mass, where Σ_u^u and Σ_d^d denote the one-loop corrections explicitly given in the Appendix of Ref. [2]. SUSY models requiring large cancellations between the various terms on the right-hand side of (1) to reproduce the measured value of M_Z^2 are regarded as unnatural, or fine-tuned.[1]

Several measures have been proposed [2–6] to quantify the degree of fine-tuning. A common feature of these is that they all regard the model to be fine-tuned if $\mu^2 \gg M_Z^2$. This is because in most models μ directly enters Eq. (1) as an *independent parameter*, and unexplained cancellations have then to be invoked to obtain the observed value of M_Z. In contrast, in most models the SSB masses are obtained in terms of one (or more) model parameters

*baer@nhn.ou.edu
†barger@pheno.wisc.edu
‡peisi@uchicago.edu
§dsmickelson@ou.edu
‖m.padeffke@ou.edu
¶tata@phys.hawaii.edu

[1]We emphasize that for superpartners up to a few TeV range the degree of fine-tuning that we are talking about is many orders of magnitude smaller than in the Standard Model because scalar masses do not exhibit quadratic sensitivity to physics at the ultrahigh scale if SUSY is softly broken.

and so are not independent, allowing for the possibility of large cancellations that is ignored by the commonly used large log measure. It is a neglect of these parameter correlations that has led some authors to conclude that light top squarks are a necessary feature of natural SUSY. In fact, as we have just argued, it is $|\mu| \sim M_Z$ and concomitantly the existence of light Higgsinos[2] (and not light stops) that is the robust conclusion of naturalness considerations. The importance of low μ for electroweak naturalness was recognized by Chan, Chattopadhyay, and Nath [8] over 15 years ago and has recently been emphasized in Refs. [2,6,9] and by Martin [10].

In earlier papers we have developed the radiatively driven natural SUSY (RNS) framework characterized by values of the parameter $\Delta_{\rm EW} = 10$–30 range corresponding to 3%–10% electroweak fine-tuning [2,6,9]. Within this framework,

(i) the superpotential μ term has magnitude $|\mu| \sim$ 100–300 GeV (the closer to M_Z the better);
(ii) the up-Higgs soft term $m_{H_u}^2$ is driven radiatively to small negative values $m_{H_u}^2(\text{weak}) \sim -M_Z^2$;
(iii) the magnitude of radiative corrections contained in Σ_u^u should be smaller than or comparable to M_Z^2. This latter condition occurs for TeV-scale highly mixed top squarks—a situation which also lifts m_h into the 125 GeV regime [6]. In contrast, the terms $m_{H_d}^2$ and Σ_d^d can occur at the multi-TeV level since they are suppressed by $\tan^2\beta$ where $\tan\beta$ is required to be in the 3–50 range.
(iv) Since the gluino mass feeds into the stop masses via renormalization group (RG) evolution—and thus into $\Sigma_u^u(\tilde{t}_{1,2})$—then low $\Delta_{\rm EW}$ also requires an upper bound on $m_{\tilde{g}} \lesssim$ 4–5 TeV [2]. Of course, M_3 is also bounded from below by the experimental bound of $m_{\tilde{g}} \gtrsim 1.3$ TeV based on LHC8 searches within the context of SUSY models like minimal supergravity model (mSUGRA)/constrained minimal supersymmetric standard model (CMSSM) [11] or within simplified models [12].
(v) First- and second-generation sfermions can be allowed anywhere in the ∼5–20 TeV range without jeopardizing naturalness [13]. The higher range of values ameliorates the SUSY flavour, *CP*, gravitino, and proton-decay problems due to decoupling.

Inspired by gauge coupling unification, in these previous studies, we had assumed gaugino mass unification as well as naturalness. From gaugino mass unification, one expects at the weak scale that $M_1 \sim M_3/7$ and $M_2 \sim 2M_3/7$ so that the LHC8 lower bound on M_3 also provides a lower bound on M_1 and M_2. In this case, for natural SUSY which respects LHC8 bounds, we expect the mass hierarchy $|\mu| < M_1 < M_2 < M_3$ to occur. Thus, in the RNS model which we take as the paradigm case for the study of natural SUSY, one expects four light Higgsino states with mass $m_{\tilde{W}_1^\pm}, m_{\tilde{Z}_{1,2}} \sim |\mu|$ where the lightest higgsino $\tilde{Z}_1$ acts as the lightest-SUSY-particle or LSP. In particular, mixed Higgsino-bino or Higgsino-wino LSPs are not allowed if the gluino is heavy.

Collider signals as well as cosmology depend sensitively on the nature of the LSP. For instance, in the RNS framework with gaugino masses near the TeV range, we expect the light electroweakinos $\tilde{W}_1^\pm$ and $\tilde{Z}_{1,2}$ to be dominantly Higgsino-like with typically small $m_{\tilde{W}_1} - m_{\tilde{Z}_1}$ and $m_{\tilde{Z}_2} - m_{\tilde{Z}_1}$ mass splittings of order 10–20 GeV [2]. Such a small mass splitting results in only soft visible energy release from the heavier Higgsino three-body decays to the $\tilde{Z}_1$. This situation makes pair production of Higgsinos very difficult to detect at LHC [14–18] in spite of their relatively small masses and correspondingly large production cross sections; other superpartners may be very heavy, and possibly beyond the reach of the LHC. In contrast, in models with light gauginos and heavy Higgsinos, the mass gap between the binolike and winolike states tends to be large (if gaugino mass unification is assumed), and signals from wino pair production followed by their decays to binolike LSPs should be readily detectable. The celebrated clean trilepton signature arising from $\tilde{W}_1\tilde{Z}_2$ production is perhaps the best-known example.

The phenomenology of dark matter is even much more sensitive to the content of the LSP. Higgsino and winolike LSPs lead to an underabundance of thermally produced LSPs, whereas a binolike LSP leads to overproduction of weakly interacting massive particles (WIMPs) unless the neutralino annihilation rate is dynamically enhanced, e.g., via an *s*-channel resonance or via coannihilation, or their density is diluted by entropy production late in the history of the Universe. In the wino- or Higgsino-LSP cases, if one solves the strong *CP* problem via a quasivisible axion [19], then the dark matter is expected to occur as an axion-neutralino admixture, i.e., two dark matter particles [20].

Gaugino mass unification—well motivated as it may be—is by no means sacrosanct. Phenomenologically, while the high scale value of M_3 is required to be large by LHC8 constraints on $m_{\tilde{g}}$, M_1 and/or M_2 may well have much smaller magnitudes without impacting naturalness. These considerations motivated us to examine how the phenomenology of natural SUSY models with $|\mu| \sim$ 100–300 GeV may be altered if we give up the gaugino mass unification assumption and allow for the possibility that the bino or/and wino also happens to be light. The LSP (and possibly also other electroweakinos) would then

[2]We assume here that there is no SUSY-breaking Higgsino mass term (such a term would lead to hard SUSY breaking—and so would be automatically forbidden—if Higgsinos had superpotential Yukawa couplings to any Standard Model singlet [7]) so that the Higgsino mass comes only from the superpotential parameter μ. This is the case in all models that we know of.

be mixtures of Higgsinos and electroweak gauginos, or may even be very nearly binolike or winolike, resulting in very different mass and mixing patterns from expectations within the RNS framework. A mixed bino-Higgsino LSP could well lead to the observed relic density for thermally produced neutralinos. We acknowledge that small values of gaugino mass parameters would have to be regarded as fortuitous from the perspective of naturalness. Nevertheless since light winos/binos do not jeopardize naturalness, in the absence of any compelling theory of the origin of SSB parameters, we felt a phenomenological study of this situation is justified by our philosophy that it is best to "leave no stone unturned" in the search for natural SUSY at the LHC.

Nonuniversal gaugino masses can occur in grand unified theory (GUT) models wherein the gauge kinetic function transforms nontrivially as the direct product of two adjoints [21,22]. Or it may be that GUTs play no role and that unification occurs within the string-model context. Models with mixed anomaly- and gravity-mediation contributions to gauginos masses also lead to nonuniversal gaugino mass parameters [23]. Investigation of how the phenomenology of natural SUSY models is modified from RNS expectations forms the subject of this paper. Naturalness in the context of nonuniversal gaugino masses has also been considered in Refs. [24] and [10].

A. Natural SUSY benchmark scenarios

We begin by exhibiting a sample benchmark point within the framework of the canonical two-extra-parameter nonuniversal Higgs model with *unified* gaugino mass parameters and a Higgsino-like LSP under the column RNSh in Table I. This point has parameters $m_0 = 5000$ GeV, $m_{1/2} = 700$ GeV, $A_0 = -8000$ GeV, and $\tan\beta = 10$ with $(\mu, m_A) = (200, 1000)$ GeV. The RNSh point has $\Delta_{\rm EW} = 9.6$ corresponding to about 10% electroweak fine-tuning, and $m_h = 124.3$ GeV while $m_{\tilde{g}} \simeq 1.8$ TeV with $m_{\tilde{q}} = 5.2$ TeV. It is safely beyond LHC8's reach. The lightest neutralino is dominantly Higgsino-like (Higgsino-wino-bino composition is listed as $v_h^{(1)} \equiv \sqrt{v_1^{(1)2} + v_2^{(1)2}}$, $v_w^{(1)}$, and $v_b^{(1)}$ defined similarly to Ref. [25]) and has mass $m_{\tilde{Z}_1} = 188$ GeV and thermally produced neutralino relic density [26] $\Omega_{\tilde{Z}_1} h^2 = 0.013$. SUSY contributions to the branching fraction for $b \to s\gamma$ are negligible so that this is close to its Standard Model (SM) value [27] and in accord with experiment [28]. The spin-independent neutralino-proton scattering cross section shown in the third-to-last row of the table naively violates the bound $\sigma^{\rm SI}(\tilde{Z}_1 p) \lesssim (2\text{–}3) \times 10^{-9}$ pb from the LUX experiment [29], but we note that this bound is obtained assuming that the neutralino comprises *all* of the cold dark matter. In our case, the thermal neutralino contribution is just about 10% of the total dark matter (DM) contribution, and this point is in accord with the constraint upon scaling the expected event rate by $\xi = \Omega_{\tilde{Z}_1} h^2/0.12$.[3] We also show the spin-dependent neutralino-nucleon scattering cross section. The IceCube experiment currently has the best sensitivity to this quantity by searching for high energy neutrinos arising from neutralinos which are captured by the Sun and annihilated in the Solar core. The current IceCube limit [31] lies around $\sigma^{\rm SD}(\tilde{Z}_1 p) \lesssim 1.5 \times 10^{-4}$ pb so that the RNSh point would seem to be excluded by this bound. For this analysis, the neutralino density in the Solar core is obtained by assuming

TABLE I. Input parameters and masses in GeV units for three natural SUSY benchmark points with $\mu = 200$ GeV and $m_A = 1000$ GeV. We also take $m_0 = 5000$ GeV, $A_0 = -8000$ GeV, and $\tan\beta = 10$. Also shown are the values of several nonaccelerator observables.

Parameter	RNSh	RNSb	RNSw
M_1(GUT)	700	380	700
M_2(GUT)	700	700	175
M_3(GUT)	700	700	700
$m_{\tilde{g}}$	1795.8	1796.2	1809.8
$m_{\tilde{u}_L}$	5116.2	5116.2	5100.7
$m_{\tilde{u}_R}$	5273.3	5271.3	5277.4
$m_{\tilde{e}_R}$	4809.0	4804.4	4806.7
$m_{\tilde{t}_1}$	1435.1	1438.1	1478.3
$m_{\tilde{t}_2}$	3601.2	3603.3	3584.9
$m_{\tilde{b}_1}$	3629.4	3631.5	3611.6
$m_{\tilde{b}_2}$	5003.9	5003.6	5007.4
$m_{\tilde{\tau}_1}$	4735.6	4731.1	4733.9
$m_{\tilde{\tau}_2}$	5071.9	5070.8	5053.9
$m_{\tilde{\nu}_\tau}$	5079.2	5078.1	5060.8
$m_{\tilde{W}_2}$	610.9	611.0	248.4
$m_{\tilde{W}_1}$	205.3	205.3	121.5
$m_{\tilde{Z}_4}$	621.4	621.5	322.1
$m_{\tilde{Z}_3}$	322.0	217.9	237.8
$m_{\tilde{Z}_2}$	209.3	209.8	211.8
$m_{\tilde{Z}_1}$	187.8	149.5	114.2
m_h	124.3	124.2	124.3
$v_h^{(1)}$	0.96	0.57	0.60
$v_w^{(1)}$	-0.14	0.07	-0.80
$v_b^{(1)}$	0.24	-0.82	0.08
$\Delta_{\rm EW}$	9.6	9.6	10.8
$\Omega_{\tilde{Z}_1}^{std} h^2$	0.013	0.11	0.0015
$BF(b \to s\gamma)$	3.3×10^{-4}	3.3×10^{-4}	3.3×10^{-4}
$\sigma^{\rm SI}(\tilde{Z}_1 p)$ (pb)	1.6×10^{-8}	1.7×10^{-8}	4.3×10^{-8}
$\sigma^{\rm SD}(\tilde{Z}_1 p)$ (pb)	1.7×10^{-4}	2.8×10^{-4}	8.9×10^{-4}
$\langle\sigma v\rangle\|_{v\to 0}$(cm^3/ sec)	2.0×10^{-25}	1.8×10^{-26}	1.7×10^{-24}

[3]We remark that other processes may further alter the neutralino relic density from its thermal value, increasing it if there are late decays of heavy particles to neutralinos or diluting it if these decay into SM particles. For more detailed discussion of nonthermally produced dark matter, see the recent review [30].

equilibration between the capture rate and the annihilation rate of neutralinos. Since the capture rate scales *linearly* with the neutralino relic density, the predicted event rates also need to be scaled by ξ before comparing with IceCube. After rescaling, we see that the RNSh point is an order of magnitude away from the IceCube upper limit of $\sim 1.5 \times 10^{-4}$ pb that is obtained assuming the neutralinos dominantly annihilate via $\tilde{Z}_1\tilde{Z}_1 \to WW$. The other columns display natural SUSY benchmark points where the bino or the wino mass parameters are dialed to relatively low values resulting in natural SUSY models with either a binolike (RNSb) or winolike (RNSw) LSP. These cases will be discussed in detail in the following sections.

B. Remainder of paper

The remainder of this paper is organized as follows. In Sec. II, we first investigate the case of $|M_1| \sim |\mu| \ll M_{2,3}$ where we treat M_1 as an additional phenomenological parameter.[4] In this case, the LSP can become mixed bino-Higgsino or even mainly binolike. Note also that, while we can always choose one of the gaugino mass parameters to be positive, the signs of the remaining ones are physical. In our study, we will examine both signs of the gaugino mass parameters that are assumed to depart from universality. In Sec. III, we investigate the case with $|M_2| \sim |\mu| \ll M_{1,3}$ which can generate a winolike LSP. In Sec. IV, we examine the more general case where both $|M_1|$ and $|M_2|$ are simultaneously comparable to $|\mu|$. Our conclusions are presented in Sec. V.

II. NATURAL SUSY WITH A BINOLIKE LSP

In this section, we examine how the phenomenology of natural SUSY models is altered if we allow for nonuniversal gaugino mass parameters and let the GUT scale bino mass vary independently. To this end, we adopt the RNSh benchmark point from Table I but now allow M_1 to be a free parameter, positive or negative. To generate spectra and the value of $\Delta_{\rm EW}$, we adopt the Isajet 7.84 spectrum generator [32]. In Fig. 1, we show by red circles the value of $\Delta_{\rm EW}$ vs the GUT scale value of M_1. We see that—aside from numerical instabilities arising from our iterative solution to the SUSY RG equations—the value of $\Delta_{\rm EW}$ stays nearly constant so that, as anticipated, varying M_1 hardly affects the degree of electroweak fine-tuning.

In Fig. 2, we show the mass values of the charginos and neutralinos as M_1 is varied between -700 GeV to 700 GeV. For $M_1 = 700$ GeV, the gaugino mass unification point, we find that $\tilde{W}_1$ and $\tilde{Z}_{1,2}$ are all Higgsino-like with mass values clustered around $\mu = 200$ GeV while the

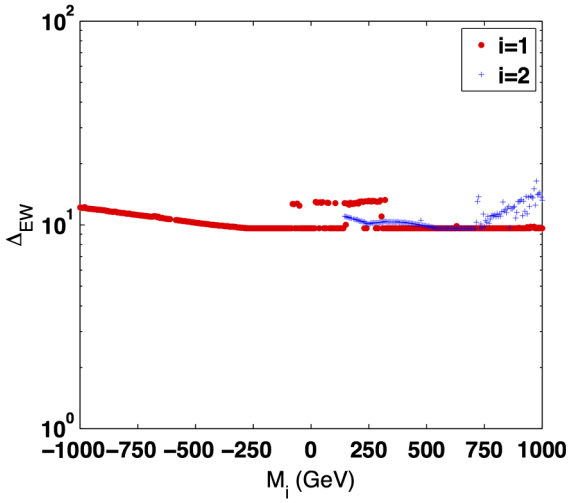

FIG. 1 (color online). Variation in fine-tuning measure $\Delta_{\rm EW}$ vs M_1 (red circles) or M_2 (blue pluses), with all other parameters fixed at their values for the RNS SUSY benchmark model point in Table I. Here and in subsequent figures, the M_i on the horizontal axis is the value of the corresponding gaugino mass parameter renormalized at the GUT scale. We cut the graphs off if the lighter chargino mass falls below 100 GeV.

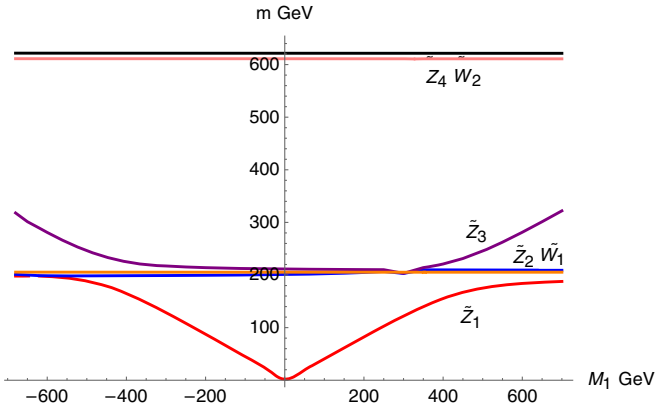

FIG. 2 (color online). Variation of electroweakino masses vs M_1 for a general RNS SUSY benchmark model with variable M_1 and $M_2 = M_3$.

binolike $\tilde{Z}_3$ lies near 300 GeV and the winolike $\tilde{Z}_4$ and $\tilde{W}_2$ lie at $\sim$600 GeV. As M_1 is lowered, the bino component of $\tilde{Z}_1$ increases while the bino component of $\tilde{Z}_3$ decreases. The mass eigenvalues track the gaugino/Higgsino content, and as we pass through $M_1 = 300$ GeV, the $\tilde{Z}_1$ and $\tilde{Z}_3$ exchange identities and interchange from being binolike to Higgsino-like. A similar level crossing is seen on the negative M_1 side of the figure. Since there is no charged bino, the values of $m_{\tilde{W}_{1,2}}$ remain constant [at μ and M_2(weak)] with variation of M_1. Since the value of $m_{\tilde{Z}_1}$ is decreasing as M_1 decreases, then the mass gaps $m_{\tilde{W}_1} - m_{\tilde{Z}_1}$ and $m_{\tilde{Z}_2} - m_{\tilde{Z}_1}$ also increase. The mass gaps reach values of $\sim$150 GeV for M_1 as small as 50 GeV. This

[4]We frequently denote both the GUT and weak scale values of the gaugino mass parameters by M_i. We assume that it will be clear from the context which case is being used so that this abuse of notation will not cause any confusion.

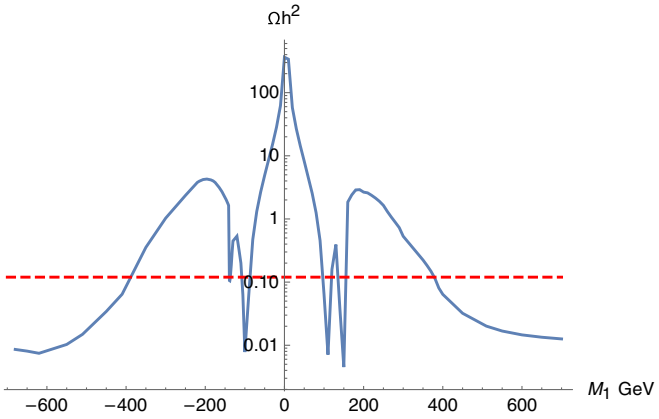

FIG. 3 (color online). Variation of $\Omega_{\tilde{Z}_1}^{\rm TP}h^2$ vs M_1 for a general RNS SUSY benchmark model with variable M_1 and $M_2 = M_3$. The dashed line shows the measured value of the cold dark matter relic density.

should render signals from $\tilde{W}_1\tilde{Z}_2$ and $\tilde{W}_1\tilde{W}_1$ production much easier to detect at the LHC as compared to the RNSh case.

In Fig. 3, we show the thermally produced neutralino relic density as calculated using the IsaReD program [26]. The value of $\Omega_{\tilde{Z}_1}h^2$ begins at ∼0.01 for $|M_1| = 700$ GeV which is typical for a Higgsino-like LSP of mass 200 GeV. As $|M_1|$ decreases, then the bino content of $\tilde{Z}_1$ becomes larger—reducing the annihilation cross section—so that the thermal relic density correspondingly increases. For $|M_1| \simeq 380$ GeV, the value of $\Omega_{\tilde{Z}_1}h^2$ reaches 0.12, i.e., it saturates the measured DM abundance, and we have the so-called well-tempered neutralino. For even lower values of $|M_1|$, then neutralinos are unable to annihilate efficiently, and $\Omega_{\tilde{Z}_1}h^2$ exceeds 1 except for special values where the neutralino annihilation cross section is resonance enhanced. For $|M_1| \sim 150$ GeV, then the binolike neutralino has mass $m_{\tilde{Z}_1} \sim m_h/2$ so that neutralinos can efficiently annihilate through the light Higgs resonance. The annihilation rate at resonance is not quite symmetric for the two signs of M_1. For even lower values of $|M_1|$, then $m_{\tilde{Z}_1} \sim M_Z/2$ so that neutralinos efficiently annihilate through the Z boson pole. At values of $|M_1| < 100$ GeV, we move below the Z resonance, and due to the increasing bino content of $\tilde{Z}_1$, the LSP annihilation cross section becomes even smaller, leading to an even larger thermal relic density.[5]

We display the SUSY spectrum for $M_1(\text{GUT}) = 380$ GeV, the value for which the thermal neutralino relic density $\Omega_{\tilde{Z}_1}^{\rm TP}h^2$ essentially saturates the measured abundance so that $\Omega_{\tilde{Z}_1}h^2 = 0.12$, in Table I as RNSb. In this case, the $\tilde{Z}_1$ is a bino-Higgsino admixture, albeit already it is dominantly binolike. The mass gap $m_{\tilde{W}_1} - m_{\tilde{Z}_1}$ is ∼56 GeV, while the mass gap $m_{\tilde{Z}_2} - m_{\tilde{Z}_1}$ is ∼60 GeV.

[5]We remind the reader that these parameter regions with seemingly too large a thermal neutralino relic density should not summarily be excluded because the neutralino relic density can be diluted if, for instance, there are heavy particles with late decays into Standard Model particles in the early Universe.

A. Implications for LHC13

The possibility of nonuniversal gaugino mass parameters has important implications for discovery of natural SUSY at LHC13.

1. *Gluino pair production:* Multijet + $E_T^{\rm miss}$ *events*

Since squarks are very heavy, the multijet + $E_T^{\rm miss}$ signal mainly arises from $pp \to \tilde{g}\tilde{g}X$ followed by gluino cascade decays mainly via $\tilde{g} \to tb\tilde{W}_j$ and $t\bar{t}\tilde{Z}_i$. For a fixed $m_{\tilde{g}}$, but varying M_1, one still expects multilepton plus multijet + $E_T^{\rm miss}$ events at a rate which mainly depends on the value of $m_{\tilde{g}}$. For discovery via gluino pair production, the LHC13 reach—which extends to about $m_{\tilde{g}} \sim 1.7$ TeV (for $m_{\tilde{g}} \ll m_{\tilde{q}}$) for 100 fb^{-1} of integrated luminosity [14]—tends to be dominated by the multijet + $E_T^{\rm miss}$ channel and so changes little compared to the case of universal gaugino masses. For the RNS point in question, the gluino dominantly decays via $\tilde{g} \to \tilde{t}_1 t$, and the $\tilde{t}_1$ subsequently decays via $\tilde{t}_1 \to b\tilde{W}_1, t\tilde{Z}_{1,2,3}$. Within the gluino pair cascade decay events, the isolated multilepton content should increase with decreasing M_1 due to the increased mass gap between $\tilde{W}_1 - \tilde{Z}_1$ and $\tilde{Z}_{2,3} - \tilde{Z}_1$ since one may also obtain energetic leptons from $\tilde{W}_1 \to \ell\nu_\ell\tilde{Z}_1$ and $\tilde{Z}_2 \to \tilde{Z}_1\ell^+\ell^-$ three-body decays in addition to those from top or $\tilde{Z}_3$ decays. If M_1 is sufficiently small, then the two-body decays $\tilde{W}_1 \to \tilde{Z}_1 W$ and $\tilde{Z}_2 \to \tilde{Z}_1 Z, \tilde{Z}_1 h$ open up. The latter two decays, if open, tend to occur at comparable rates in natural SUSY with a binolike LSP since the lighter -inos tend to be a gaugino-Higgsino admixture. The isolated opposite-sign/same-flavor (OS/SF) dileptons present in cascade decay events will have mass edges located at $m_{\tilde{Z}_2} - m_{\tilde{Z}_1}$ for three-body decays, or else real $Z \to \ell^+\ell^-$ or $h \to b\bar{b}$ pairs will appear in the case of two-body decays of $\tilde{Z}_2$ and $\tilde{Z}_3$.

2. *Electroweakino pair production*

For electroweakino pair production, allowing nonuniversality in the gaugino sector changes the situation quite dramatically. In the case of RNS with gaugino mass unification, the Higgsino pair production reactions $pp \to \tilde{W}_1^+\tilde{W}_1^-$ and $\tilde{W}_1\tilde{Z}_{1,2}$ are largely invisible due to the small mass gaps [14]. It may, however, be possible to detect Higgsino pair production making use of initial state QCD radiation and specially designed analyses if the Higgsino mass is below ∼170–200 GeV, depending on the integrated luminosity [17,18].

The wino pair production process $pp \to \tilde{W}_2\tilde{Z}_4X$ can lead to a characteristic same-sign diboson signature [33] arising from $\tilde{W}_2^{\mp} \to \tilde{Z}_1W^{\mp}$ and $\tilde{Z}_4 \to \tilde{W}_1^{\pm}W^{\mp}$ decays, where the Higgsinos decay to only soft visible energy and are largely invisible.

In contrast, as M_1 diminishes, then the growing $\tilde{W}_1 - \tilde{Z}_1$ and $\tilde{Z}_2 - \tilde{Z}_1$ mass gaps give rise increasingly to visible decay products and a richer set of electroweakino signals. In Fig. 4, we show the next-to-leading-order (NLO) cross sections obtained using Prospino [34] for various electroweakino pair production reactions vs variable $M_1(GUT)$ for the RNS benchmark case.[6] As M_1 falls to lower values, the chargino pair rates remain constant since μ and M_2 do not change. The $\tilde{W}_1\tilde{W}_2$ cross section in the topmost frame is small because squarks are very heavy, and the $Z\tilde{W}_1\tilde{W}_2$ coupling is dynamically suppressed. Although the $\tilde{W}_1 \to f\bar{f}'\tilde{Z}_1$ decay products become more energetic with reducing $|M_1|$, the chargino pair signals are typically challenging to extract from large SM backgrounds such as W^+W^- production.

For $\tilde{W}_1\tilde{Z}_{1,2}$ production, the cross sections can be large, but the decays give only soft visible energy for $M_1 \sim 700$ GeV. But as M_1 is lowered, the cross section for $\tilde{W}_1\tilde{Z}_2$ remains, large but the mass gaps increase. Ultimately, the clean trilepton signature should become visible against SM backgrounds [35,36]. Also, the reaction $pp \to \tilde{W}_1\tilde{Z}_3$ has an increasing cross section as M_1 decreases and should give rise to $\ell + Z$ events: trileptons where one pair reconstructs a real Z [37], as is the case for the RNSb benchmark point; see also Refs. [38,39]. Ultimately, the $\tilde{Z}_3 \to \tilde{Z}_1h$ mode also opens up, reducing the trilepton signal but potentially offering an opportunity for a search via the Wh channel [40].

In models with heavy squarks, Higgsino pair production reactions make the main contribution to neutralino pair production processes. In many models, $|\mu|$ is large, making neutralino pair production difficult to see at hadron colliders. Natural SUSY models with nonuniversal gaugino masses are an exception as can be seen from the bottom frame of Fig. 4 where we show cross sections for various neutralino pair production processes. The bino-Higgsino level crossing that we mentioned earlier is also evident: for large M_1, the $\tilde{Z}_1$ and $\tilde{Z}_2$ are Higgsino-like states, and $\tilde{Z}_1\tilde{Z}_2$ production (solid squares) dominates, whereas for small M_1, then $\tilde{Z}_2$ and $\tilde{Z}_3$ are Higgsino-like, and $\tilde{Z}_2\tilde{Z}_3$ production (left-pointing triangles) is dominant even though the $\tilde{Z}_1\tilde{Z}_2$ and $\tilde{Z}_1\tilde{Z}_3$ reactions are kinematically favored. Also $\tilde{Z}_1\tilde{Z}_2$ and $\tilde{Z}_2\tilde{Z}_3$ production can lead to dilepton and four-lepton final states, which may be visible, and to ZZ, Zh and $hh + E_T^{\rm miss}$ final states if $|M_1|$ is sufficiently small.

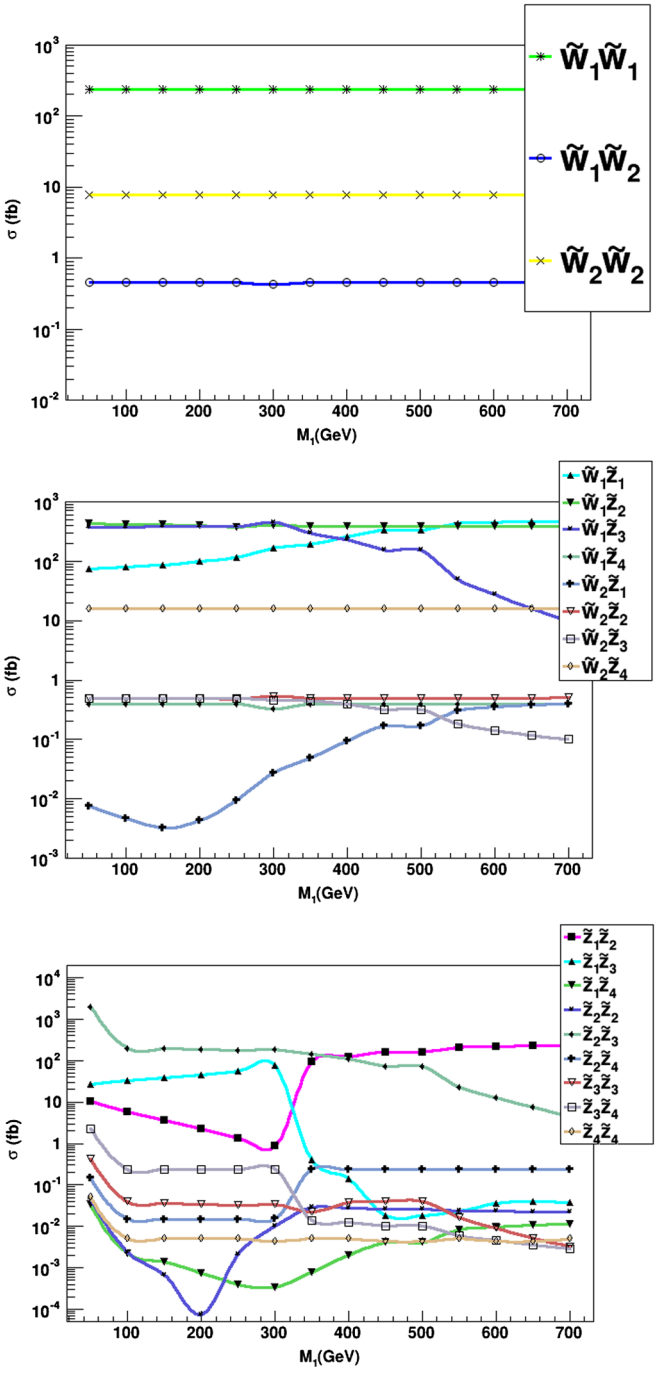

FIG. 4 (color online). Electroweakino pair production cross sections vs M_1 for the RNS SUSY benchmark model with variable M_1 but with $M_2 = M_3$.

B. Implications for ILC physics

The prospects for SUSY discovery and precision measurements in the RNS model have been examined for an International Linear e^+e^- Collider (ILC) with $\sqrt{s} \sim 250$–1000 GeV in Ref. [41]. Such a machine is a

[6]Since, as we saw in the previous figures, the mixing patterns are roughly symmetric about $M_1 = 0$, and because it is relatively time consuming to run Prospino, we show results only for positive values of M_1.

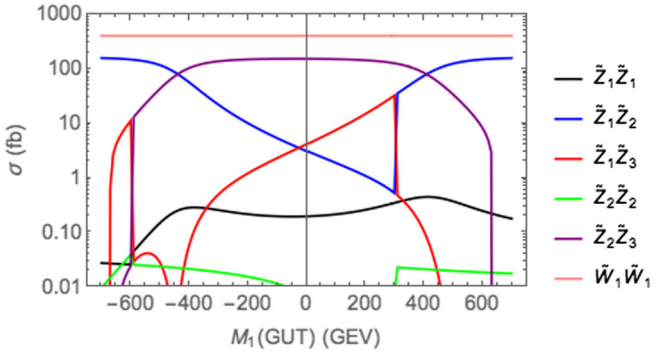

FIG. 5 (color online). Chargino and neutralino production cross sections at a linear e^+e^- collider with $\sqrt{s} = 500$ GeV with unpolarized beams for the RNS SUSY benchmark model with variable M_1 but with $M_2 = M_3$.

Higgsino factory in addition to a Higgs factory, and even with small (10 GeV) inter-Higgsino mass gaps, SUSY signals should stand out above SM backgrounds. The clean environment, together with the availability of polarized electron beams, also allows for precision measurements that point to the Higgsino origin of these events. The main reactions of import are $e^+e^- \to \tilde{W}_1^+\tilde{W}_1^-$ and $\tilde{Z}_1\tilde{Z}_2$ production.

In the case where M_1 is low enough so that one obtains a binolike LSP, the second Higgsino state $\tilde{Z}_3$ also becomes accessible, and reactions involving $\tilde{Z}_3$ provide even richer prospects for SUSY discovery. Various SUSY pair production cross sections are shown in Fig. 5 vs variable M_1 and for $\sqrt{s} = 500$ GeV. The electron and positron beams are taken to be unpolarized in this figure. Once again the level crossings between binolike and Higgsino-like states are evident. For the case of unified gaugino masses with $M_1 = 700$ GeV, then indeed only $\tilde{W}_1\tilde{W}_1$ and $\tilde{Z}_1\tilde{Z}_2$ are available. However, as $|M_1|$ is lowered, then $\sigma(\tilde{W}_1\tilde{W}_1)$ remains constant although the decay products of $\tilde{W}_1$ become more energetic once the LSP becomes binolike and lighter than the Higgsino. The dijet mass spectrum from $\tilde{W}_1 \to \tilde{Z}_1 q\bar{q}'$ decay allows for precision extraction of $m_{\tilde{W}_1}$ and $m_{\tilde{Z}_1}$ and also extraction of the weak scale SUSY parameters μ and also M_1, if the bino mass is small enough [41–43].

Turning to neutralino production, we see that Higgsino pair production—$\tilde{Z}_1\tilde{Z}_2$ production if $|M_1|$ is large and $\tilde{Z}_2\tilde{Z}_3$ production for small values of $|M_1|$—dominates the neutralino cross section just as in the LHC case. Notice that for $0 < M_1 < 300$ GeV $\tilde{Z}_1\tilde{Z}_3$ production also occurs at an observable rate, falling with reducing M_1 because of the increasing bino content of $\tilde{Z}_1$.[7] We have checked that the strong dip in $\sigma(\tilde{Z}_1\tilde{Z}_3)$ around $M_1 \simeq 500$ GeV is due to an accidental cancellation in the $Z\tilde{Z}_1\tilde{Z}_3$ coupling.[8] $\tilde{Z}_2\tilde{Z}_3$ and $\tilde{Z}_1\tilde{Z}_3$ production should lead to interesting event topologies, including $Z + E_T^{\rm miss}$ and $h + E_T^{\rm miss}$ events where the missing mass does *not* reconstruct to M_Z, depending on the decay modes of the neutralinos. On the negative M_1 side, the $\tilde{Z}_1\tilde{Z}_3$ cross section is small, except beyond the level crossing at $M_1 \simeq -600$ GeV.

Before closing, we note that these neutralino and chargino cross sections are also sensitive to beam polarization. This can serve to extract the gaugino/Higgsino content of the charginos and neutralinos that are being produced.

C. Implications for dark matter seaches

In the RNS model with unified gaugino masses and a Higgsino-like LSP, the relic density of thermally produced neutralinos is much smaller than the observed density of cold dark matter. This allows for a contribution from axions [19] that must be present if nature adopts the Peccei–Quinn solution to the strong *CP* problem. In the case of Dine-Fischler-Srednicki-Zhitnitsky axions [44], one also gains a solution to the SUSY μ problem and can allow for a natural value of $\mu \sim 100$–200 GeV via radiative Peccei-Quinn breaking [45]. In such models, the DM tends to be axion dominated [46] with a local abundance of neutralino WIMPs reduced by factors of 10–15 from usual expectations. The reduced local abundance makes direct detection more difficult since detection rates depend linearly on the local neutralino abundance. Indirect detection rates from WIMP halo annihilations depend on the square of the local abundance and so are even more suppressed in models where the WIMPs only make up a fraction of the dark matter [47].

For the more general model where $|M_1|$ may be lower than expected from gaugino mass unification, the thermally produced neutralino abundance is increased, and consequently one expects a greater fraction of neutralino dark matter compared to axions, assuming there are no other processes that affect the neutralino relic density. The increased local neutralino abundance leads to more favorable prospects for WIMP direct and indirect detection.

The spin-independent (SI) WIMP-proton scattering cross section from IsaReS [48] is shown in Fig. 6. The curve with red dots shows the case of variable M_1. As M_1 decreases

[7]This is somewhat different from the behavior in Fig. 4 where we see, for example, that $\sigma(\tilde{Z}_1\tilde{Z}_2)$ increases with reducing M_1. We attribute this to the reduction in mass of the $\tilde{Z}_1\tilde{Z}_2$ system and the concomitant increase of the parton densities at the LHC.

[8]The alert reader may wonder why there is no similar dip in Fig. 4. We remark that the code used to make Fig. 5 uses tree-level masses and mixings among charginos and neutralinos, whereas Fig. 4 includes effects of radiative corrections to the spectrum. These corrections, of course, shift the location as well as depth of the dip. We have checked that the coupling is indeed suppressed even with radiative corrections, but there is no big dip, at least within the resolution of the scan. Since it has no implications physics-wise because $\sigma(\tilde{Z}_1\tilde{Z}_3)$ in Fig. 4 is already very small for $M_1 \sim 500$ GeV, we have not attempted to refine this figure.

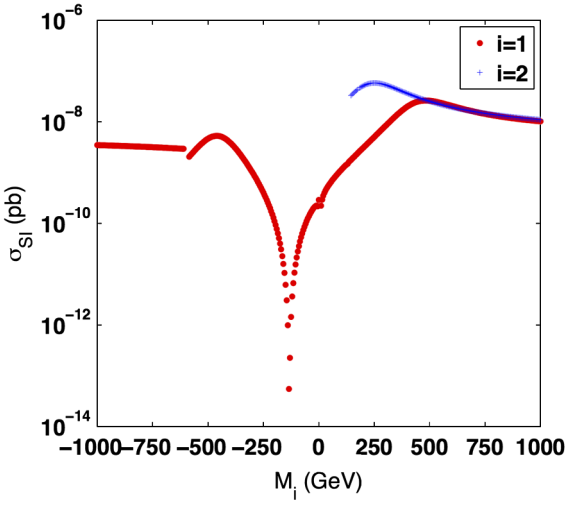

FIG. 6 (color online). Spin-independent $p\tilde{Z}_1$ scattering cross section vs M_1 (red dots) or M_2 (blue pluses) for the RNS benchmark point.

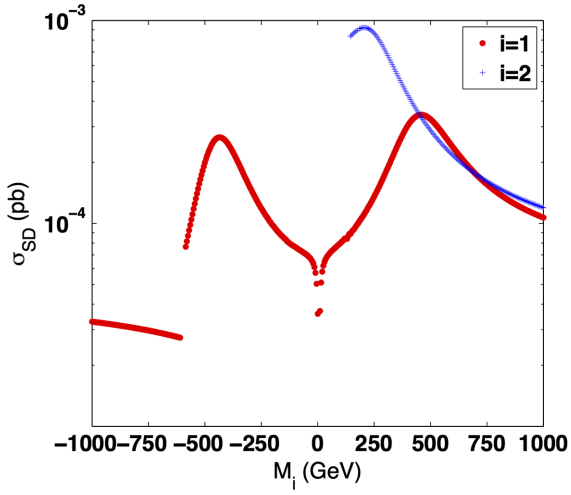

FIG. 7 (color online). Spin-dependent $p\tilde{Z}_1$ scattering cross section vs M_1 (red circles) or M_2 (blue pluses) for the RNS benchmark point.

from large, positive values, then the LSP becomes more of a bino-Higgsino admixture. Since the SI cross sections proceed mainly through light Higgs h exchange, and the Higgs-neutralino coupling is proportional to a product of gaugino times Higgsino components [25], then the SI direct detection cross section increases by up to a factor of ∼2 for lowered M_1. As M_1 is lowered even further, then the LSP becomes more purely binolike, and the SI direct detection cross section drops sharply. The sharp dip at $M_1 \simeq -110$ GeV is due to the reduction of the $h\tilde{Z}_1\tilde{Z}_1$ coupling and also the cancellation between the neutralino scattering through the exchange of the light CP-even Higgs and that through the exchange of the heavy CP-even Higgs, denoted as the blind spot in dark matter direct detection [25,49,50]. The kink at $M_1 \sim -600$ GeV occurs due to a change in the composition of the LSP; we see from Fig. 2 that the levels are getting very close, and the -inos may be switching composition.

The reader may be concerned that the cross section in Fig. 6 seemingly violated the upper limits from LUX (Ref. [29]) of $\sim(1\text{–}2) \times 10^{-9}$ pb for neutralinos in the mass range 20–200 GeV. As mentioned previously, we should remember that these limits assume that the LSP saturates the observed density of cold dark matter, which is certainly *not the case* for a Higgsino-like LSP (large $|M_1|$ values in the figure). Re-scaling the expected event rate by the fractional relic density makes the large $|M_1|$ region safe —though on the edge of observability—to LUX constraints (which otherwise assume that neutralinos saturate the measured density of cold dark matter). For smaller values of $|M_1|$, where it may also appear that the direct detection bound is violated, this clearly is not the case. We should, however, keep in mind that for these ranges of M_1 the direct detection rate from which the bound in Ref. [29] is inferred cannot be reliably calculated because the physics processes responsible for bringing the neutralino relic density to its final value lie outside the present framework. Put differently, we caution against unilaterally excluding model parameters (including the RNSb model) based on these considerations because this frequently requires other assumptions about the cosmological history of the Universe that have no impact upon collider physics.[9] While WIMP discovery would be unambiguous, interpretation of the physics underlying any signal would require a careful specification of all underlying assumptions.

The expected spin-dependent (SD) proton-neutralino direct detection cross section is plotted vs the gaugino mass parameter in Fig. 7. In this case, the scattering occurs dominantly via Z exchange. The $Z\tilde{Z}_1\tilde{Z}_1$ coupling (Eq. (8.101) of Ref. [25]) is proportional to a difference in square of Higgsino components of the neutralino. For M_1 large and positive, both Higgsino components are comparable, and there is a large cancellation in the coupling. As M_1 decreases, the Higgsino components of $\tilde{Z}_1$ decrease, the up-type Higgsino content more so than the down type. There is less cancellation, and the coupling increases. As M_1 decreases further, the bino component increases, and the smallness of the Higgsino components decreases the coupling. The negative M_1 side shows similar features until we reach $M_1 \simeq -600$ GeV where the flip in the identity of the neutralino mentioned in the previous figure results in the discontinuity.

As far as WIMP detection goes, the SD cross section would influence IceCube [31] detection rates the most since the WIMP abundance in the solar core is determined by equilibration between the capture rate and the annihilation

[9]What is clear from the data is that neutralinos with a large Higgsino content (including the well-tempered neutralino) cannot be the bulk of the local dark matter.

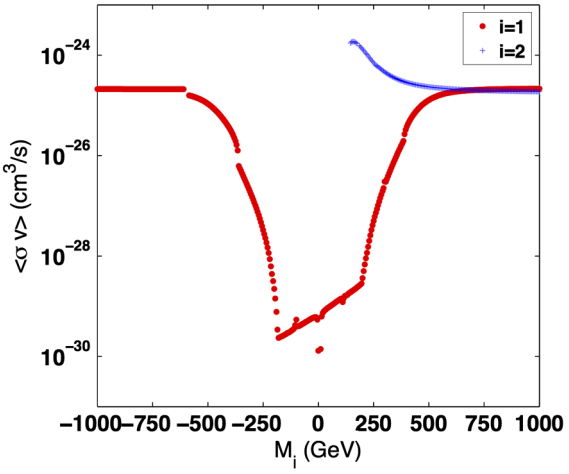

FIG. 8 (color online). Thermally averaged neutralino annihilation cross section times velocity at $v = 0$ vs M_1 (red dots) or M_2 (blue pluses) for the RNS benchmark point.

rate of WIMPs in the Sun. The scattering/capture rate of the Sun depends mainly on the hydrogen-WIMP scattering cross section which proceeds more through the SD interaction since there is no nuclear mass enhancement. While some of the predicted values (red points) might well be marginally excluded by the IceCube search, the takeaway message is that for the most part the model with $\mu = 200$ GeV is on the edge of detectability, as long as neutralinos dominantly annihilate to W pairs and assuming that neutralinos essentially saturate the entire cold dark matter relic density.

In Fig. 8, we show the thermally averaged neutralino annihilation cross section times relative velocity evaluated as $v \to 0$. This quantity enters the halo WIMP annihilation rate, and detection rate for galactic positrons, antiprotons, and gamma rays from WIMP halo annihilations are proportional to this factor. In the case of gaugino mass unification where we have a Higgsino-like neutralino, then the local abundance is reduced, and the expected detection rate is reduced by the square of the WIMP underabundance: ξ^2 where $\xi = \Omega_{\tilde{Z}_1} h^2/0.12$. From the figure, we see that, while the local abundance increases as $|M_1|$ is reduced (Fig. 3), the annihilation rate decreases because annihilation to WWs occurs mainly via the (reducing) Higgsino component of the LSP. Once this channel is closed (around $|M_1| \simeq 200$ GeV), annihilation to fermions takes over, and the rate drops further. The FERMI-LAT Collaboration has obtained upper limits located at about a few $\times 10^{-26}$ cm^3/s ($\sim 2 \times 10^{-25}$ cm^3/s) for annihilation to $b\bar{b}$ (WW pairs) [51]. Assuming a Navarro–Frenk–White profile for dwarf galaxies in the analysis, models with a larger cross section would have led to a flux of gamma rays not detected by the experiment. Even without the ξ^2 scaling noted above, and certainly after the scaling, these bounds do not exclude any of the points in the figure. For completeness we note that all the caveats that we discussed for the applicability of direct detection bounds are also applicable in this case, and we urge the reader to use caution in excluding ranges of parameters even if the Fermi Collaboration obtains tighter bounds in the future.

III. NATURAL SUSY WITH A WINOLIKE LSP

In this section, we examine the phenomenological implications of altering the $SU(2)$ gaugino mass parameter M_2 while keeping $M_1 = M_3 = 700$ GeV. We begin by showing, as blue pluses, the variation of $\Delta_{\rm EW}$ with M_2 in Fig. 1. Again, we see that $\Delta_{\rm EW}$ is relatively insensitive to M_2 except for the largest values of this parameter. This is due to the increasing contribution of winos to $\Sigma_u^u(\tilde{W}_{1,2})$. Thus, models with $M_2 \ll M_{1,3}$ lead to a winolike LSP at little cost to naturalness. For $M_2 < 150$ GeV, the chargino becomes lighter than 100 GeV (roughly the chargino mass bound from LEP2). Here, and in subsequent figures, we do not consider negative values of M_2 as these lead to a chargino LSP: $m_{\tilde{W}_1} < m_{\tilde{Z}_1}$.

In Fig. 9, we show how the masses of charginos and neutralinos change as M_2 is reduced from its unified value. Starting with the RNSh spectra at $M_2 = 700$ GeV, where the $\tilde{W}_2$ and $\tilde{Z}_4$ are essentially winos, and $\tilde{Z}_1$, $\tilde{Z}_2$, and $\tilde{W}_1$ are Higgsinos, we see that, as M_2 is lowered, the mass of the winolike states reduces, whereas the Higgsino-like states remain with the mass fixed close to μ. The mass of the binolike $\tilde{Z}_3$ also remains nearly constant. This behavior persists until we reach the bino-wino level crossing near $M_2 \simeq 350$ GeV where $\tilde{Z}_3$ and $\tilde{Z}_4$ switch identities. For still lower values of M_2, we see another level crossing between the charged as well as neutral winolike and Higgsino-like states. For $M_2 < 200$ GeV, the lighter chargino as well as the LSP are winolike, the heavier chargino and the neutralinos $\tilde{Z}_{2,3}$ are Higgsino-like, and $\tilde{Z}_4$ is mainly a bino. The mass gap $m_{\tilde{W}_1} - m_{\tilde{Z}_1}$ has actually decreased with decreasing M_2 since these winolike states have very tiny

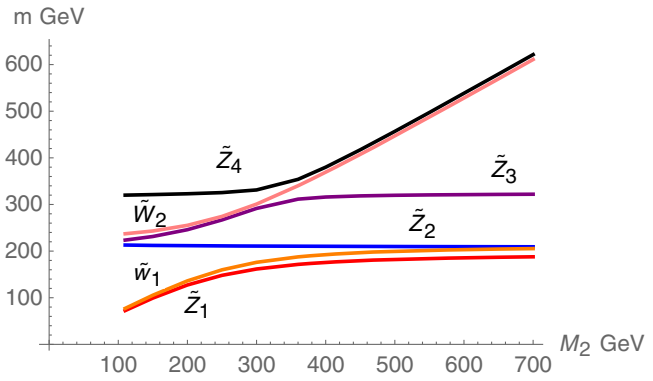

FIG. 9 (color online). Variation of chargino and neutralino masses vs M_2 for the RNS SUSY benchmark model with variable M_2 but with $M_1 = M_3$.

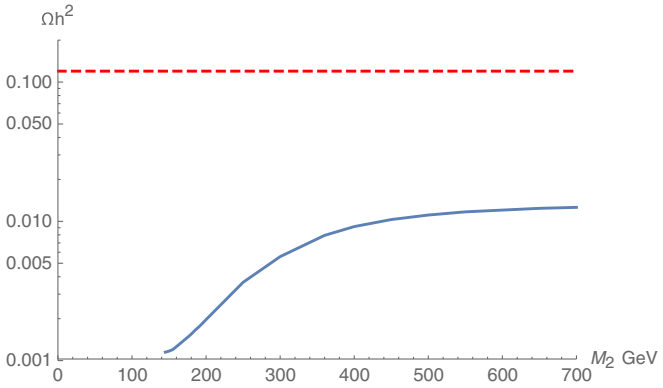

FIG. 10 (color online). Variation of $\Omega_{\tilde{Z}_1}^{\rm TP}h^2$ vs M_2 (blue curve) for the RNS SUSY benchmark model with variable M_2 but with $M_1 = M_3$. We cut the graph off at the low end because $m_{\tilde{W}_1}$ falls below its LEP2 bound.

mass splittings. The mass gaps $m_{\tilde{W}_2} - m_{\tilde{Z}_1}$ and $m_{\tilde{Z}_2} - m_{\tilde{Z}_1}$ greatly *increase* with decreasing M_2, reflecting the widening Higgsino-wino mass difference. This should make their visible decay products harder so that these states are easier to detect at the LHC.

We show the thermally produced neutralino relic density $\Omega_{\tilde{Z}_1}h^2$ vs M_2 in Fig. 10. Starting with $M_2 = 700$ GeV for which $\Omega_{\tilde{Z}_1}h^2 \sim 0.01$, we see that $\Omega_{\tilde{Z}_1}h^2$ steadily decreases with decreasing M_2 and reaches a value $\Omega_{\tilde{Z}_1}h^2 \sim 0.001$ for very low values of M_2 where the $\tilde{Z}_1$ is nearly pure wino. This is because wino annihilation proceeds via the larger SU(2) triplet coupling to electroweak gauge bosons while annihilation of Higgsinos proceeds via the smaller doublet coupling—the cross section for annihilation to W pairs, which is dominated by the t-channel chargino exchange, goes as the fourth power of this coupling. Thus, in the case of low M_2 with a winolike neutralino, we might expect an even more reduced local abundance from *thermally produced LSPs*. The balance may be made up either by axions or other relics, or by LSPs produced by late decays of heavier particles. We cut the graph off when $m_{\tilde{W}_1}$ falls below its LEP2 bound. We do not see any dips corresponding to s-channel h or Z funnel annihilation as these fall in the LEP2 excluded region.

An RNS benchmark point with a winolike LSP is shown in Table I and is labelled as RNSw. All input parameters for RNSw are the same as for RNSh except now M_2 is chosen to be 175 GeV. The $\tilde{W}_1 - \tilde{Z}_1$ mass gap has decreased to just 7.3 GeV, while the $\tilde{Z}_2 - \tilde{Z}_1$ mass gap has increased beyond the RNSh value up to ~97 GeV, large enough so that both $\tilde{Z}_2 \to \tilde{Z}_1 Z$ and $\tilde{Z}_2 \to \tilde{W}_1^{\pm} W^{\mp}$ decays are now allowed. In such a scenario, we would expect LHC SUSY cascade decay events to be rich in content of real Z bosons that could be searched for at the LHC. In fact, the CMS [52] and ATLAS [53] collaborations have already obtained bounds on chargino and neutralino masses from an analysis of about 20 fb^{-1} of LHC8 data. These limits are obtained in simplified models from an analysis of expectations from $\tilde{W}_1\tilde{Z}_2$ and $\tilde{W}_1\tilde{W}_1$ production at LHC8, assuming that $m_{\tilde{W}_1} = m_{\tilde{Z}_2}$ and that the charginos (neutralinos) decay 100% of the time to W bosons (Z bosons or Higgs bosons). The ATLAS bound [53]—obtained from a combination of the dilepton and trilepton channels—excludes wino pair production for wino masses up to 250 (400) GeV provided the LSP is lighter than 100 (150) GeV, while the current CMS limit is considerably less restrictive. While these limits are not directly applicable to pair produced $\tilde{W}_1$ and $\tilde{Z}_2$ for the RNSw scenario in the table, the reader may be concerned that *Higgsino-pair production* processes $pp \to \tilde{W}_2\tilde{Z}_{2,3}X, \tilde{W}_2\tilde{W}_2X$ would lead to final states similar to those that the LHC searches look for. It is clear that the RNSw scenario, with $m_{\tilde{Z}_1} = 114$ GeV, is clearly allowed by current searches; aside from the fact that the LSP mass exceeds 100 GeV for which there is no LHC limit, the Higgsino pair production cross section is smaller than that for wino pair production. This will further weaken the bound for the RNSw case. Data from the LHC13 run should, however, decisively probe this benchmark point.

A. Implications for LHC13

1. Gluino pair production: Multijet plus $E_T^{\rm miss}$ events

As discussed in Sec. II A 1, the discovery reach of LHC13 for gluino pairs mainly depends on the value of $m_{\tilde{g}}$ which dictates the total $\tilde{g}\tilde{g}$ production cross section in the case of heavy squarks. We would thus expect a similar LHC13 reach for gluino pair production in the RNSw case as for RNSh and as for mSUGRA/CMSSM for comparable gluino masses and heavy squarks. Also, in the RNSw case, then charginos $\tilde{W}_1$ will still be largely invisible due to their soft decay products. In some anomaly-mediated SUSY breaking models with a winolike LSP, then the mass gap $m_{\tilde{W}_1} - m_{\tilde{Z}_1}$ lies at the 100 MeV level leading to long-lived winos of which the tracks before decay may be visible [54]. In our case though, since μ is 100–200 GeV as required by naturalness, the $\tilde{W}_1 - \tilde{Z}_1$ mass gap tends to lie in the 5–10 GeV range, and so charged winos will be short-lived with no discernable tracks or kinks. However, in the RNSw case, then the $\tilde{Z}_2 - \tilde{Z}_1$ mass gap does become large, and the well-known dilepton mass edge at $m_{\tilde{Z}_2} - m_{\tilde{Z}_1}$ should be observable for energetic enough $\tilde{Z}_2 \to \tilde{Z}_1 \ell^+\ell^-$ decays if $m_{\tilde{Z}_2} - m_{\tilde{Z}_1} < M_Z$. In the case where the decay $\tilde{Z}_2 \to \tilde{Z}_1 Z$ opens up, then the gluino cascade decay events (which, depending on the spectrum, should mostly proceed via real or virtual stop decays because stops are much lighter than first-/second-generation squarks) should be rich in OS/SF dileptons which reconstruct M_Z. Note also that for modest values of M_2 $\tilde{Z}_3$ is also expected to be relatively light and should also be accessible via gluino decays. For yet smaller

values of M_2, $\tilde{Z}_{2,3} \to \tilde{Z}_1 h$ may also be allowed and should occur with a comparable branching fraction to the decay to real Zs.

2. Electroweakinos at LHC13

In Fig. 11, we show NLO cross sections from Prospino [34] for electroweakino pair production at LHC13 for the RNS benchmark but for variable M_2. Chargino pair production—shown in the topmost frame—occurs via wino as well as via Higgsino pair production. For large M_2, the latter dominates, but as M_2 is reduced, wino pair production increases in importance until it completely dominates for $M_2 \sim 100$ GeV. $\tilde{W}_1\tilde{W}_2$ production for the most part occurs via small gaugino/Higgsino content and so has a smaller cross section than the kinematically disfavored $\tilde{W}_2\tilde{W}_2$ production. The level crossing as the light chargino transitions from being Higgsino-like to winolike as M_2 reduces is also evident in the upper two curves.

Chargino-neutralino production, shown in the middle frame, also occurs via wino as well as Higgsino-pair production processes. For large values of M_2, Higgsino pair production dominates, and $\tilde{W}_1\tilde{Z}_{1,2}$ production processes have the largest cross sections. For very small values of M_2, pair production of winos is dynamically and kinematically favored, and $\tilde{W}_1\tilde{Z}_1$ occurs at the highest rate. The Higgsino-like states $\tilde{W}_2, \tilde{Z}_{2,3}$ have masses μ and are also produced with substantial cross sections. Notice that $\tilde{W}_1\tilde{Z}_2$ production remains significant even for small values of M_2, presumably because it is favored by kinematics (and increased parton luminosity).

Neutralino pair production (shown in the bottom frame) can only occur via Higgsino pair production since electroweak gauge invariance precludes a coupling of Z to neutral gauginos. As a result, $\tilde{Z}_1\tilde{Z}_2$ production dominates for large M_2. For small values of M_2 (where $\tilde{Z}_1$ becomes winolike), $\tilde{Z}_2\tilde{Z}_3$ production becomes important; however, $\tilde{Z}_1\tilde{Z}_2$ production remains large because of large parton densities.

We see that for $M_2 \lesssim 300$ GeV the cross sections for $\tilde{W}_1\tilde{Z}_1$ and $\tilde{W}_1\tilde{W}_1$ production processes increase rapidly with decreasing M_2 since $\tilde{W}_1$ and $\tilde{Z}_1$ become increasingly winolike. However, since the $\tilde{W}_1 - \tilde{Z}_1$ mass gap reduces even below the Higgsino-LSP case, these states remain difficult—perhaps impossible—to detect. Possibly $\tilde{W}_1\tilde{W}_1$ production may be detectable via vector-boson-fusion-like cuts in events where energetic jets with a large rapidity gap are required [55]. Although the cross section for winolike $\tilde{W}_1\tilde{Z}_1$ production becomes very large at low M_2, this process is difficult to detect. However, $\tilde{W}_1\tilde{Z}_2$ production remains at viable rates even for low M_2. In this case, one might look for relatively hard OS/SF dileptons from $\tilde{Z}_2$ decay recoiling against only soft tracks and $E_T^{\rm miss}$. Other possibly more promising reactions at low M_2 include

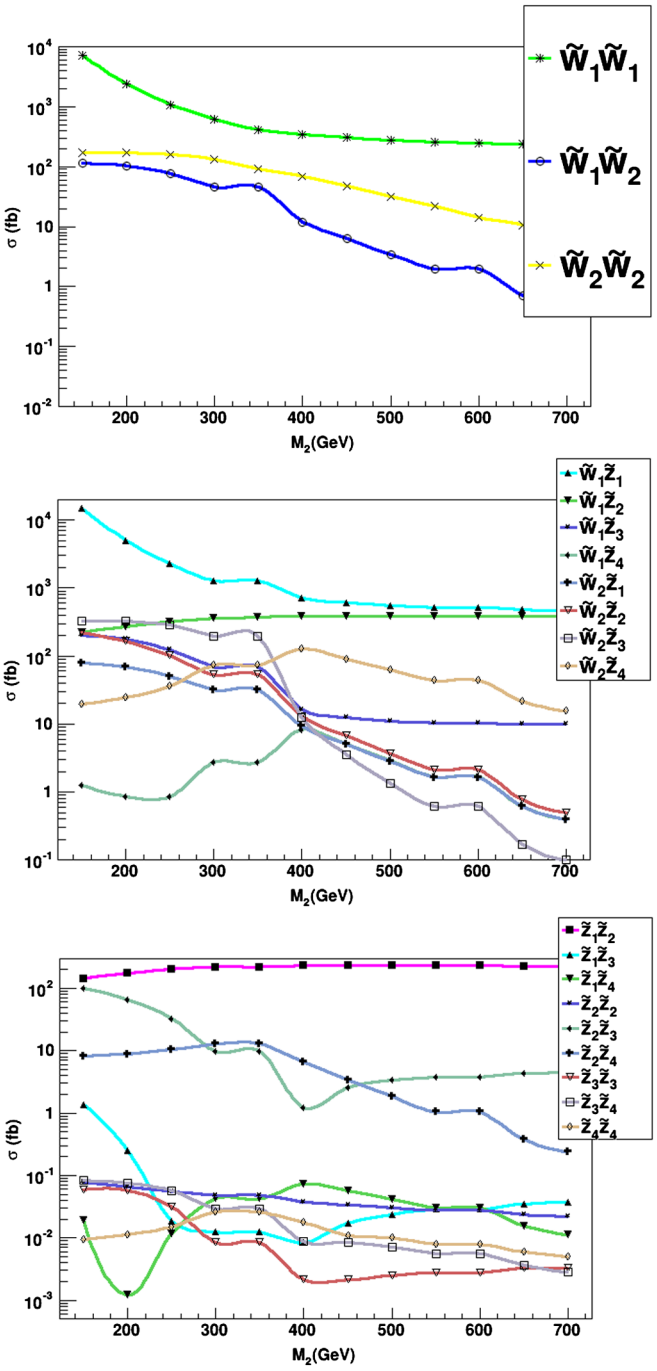

FIG. 11 (color online). Electroweakino pair production cross sections vs M_2 for the RNS SUSY benchmark model with variable M_2 but with $M_1 = M_3$.

$\tilde{W}_2\tilde{Z}_3$, $\tilde{W}_2\tilde{Z}_2$, $\tilde{Z}_2\tilde{Z}_3$, and maybe also $\tilde{Z}_2\tilde{Z}_4$ production, since the decay products from both the chargino and neutralino should be relatively hard and can lead to $E_T^{\rm miss}$ events with three or more leptons, or real Z and Higgs bosons. As we mentioned, LHC collaborations are already searching for an excess of just such events [52,53,56]. Constraints from $Wh + E_T^{\rm miss}$ analyses are currently much weaker than those from the $WZ + E_T^{\rm miss}$

analyses discussed above. Note also that $\tilde{W}_1\tilde{Z}_3$ and $\tilde{Z}_1\tilde{Z}_2$ production each has a cross section in excess of 100 fb at low M_2 but would be considerably more difficult to detect.

B. Implications for ILC

At the ILC, the natural SUSY scenario with low M_2 becomes both more challenging and richer. The cross sections for chargino and neutralino pair production at ILC500 are shown in Fig. 12 for unpolarized beams. For $M_2 = 700$ GeV, we have the Higgsino pair production reactions $e^+e^- \to \tilde{W}_1^+\tilde{W}_1^-$ and $\tilde{Z}_1\tilde{Z}_2$ dominating. As M_2 is lowered, then the $\tilde{W}_1$ becomes more winolike and lighter leading to a larger cross section. However, the mass gap $\tilde{W}_1 - \tilde{Z}_1$ drops below 10 GeV, making chargino pairs more difficult but likely still possible to detect with specially designed cuts. Beam polarization would serve to ascertain the Higgsino/wino content of the chargino. Also, the $\tilde{Z}_1\tilde{Z}_2$ reaction falls with decreasing M_2 as the $Z - \tilde{Z}_1 - \tilde{Z}_2$ coupling decreases (Z only couples to Higgsino components). As M_2 falls below 300 GeV, the $\tilde{Z}_2\tilde{Z}_3$ reaction turns on and grows in importance because the $\tilde{Z}_3$ becomes increasingly Higgsino-like. Here, we expect $\tilde{Z}_3$ to decay via two-body modes into Z-bosons or Higgs bosons and $\tilde{Z}_2$ to decay either to two- or three-body modes depending on the mass gap. This reaction should be distinctive and easily visible.

C. Implications for WIMP detection

WIMP detection for models with radiatively driven naturalness and a winolike WIMP may be either more and less difficult than the case with gaugino mass unification since, though the nucleon neutralino scattering cross section is larger, the local abundance for a thermally produced winolike LSP is below the already low value typical of a Higgsino-like LSP. Of course, the thermal wino abundance can be augmented by nonthermal processes

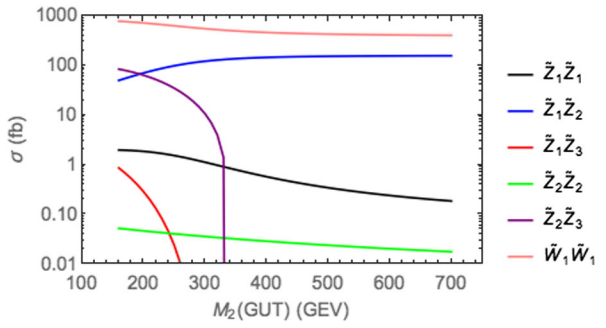

FIG. 12 (color online). Chargino and neutralino production cross sections with unpolarized electron and positron beams at a linear e^+e^- collider with $\sqrt{s} = 500$ GeV for the RNS SUSY benchmark model with variable M_2 but with $M_1 = M_3$.

involving moduli decay [57] or axino/saxion decay [30] in the early Universe.

In Fig. 6 we show the SI direct detection $\tilde{Z}_1 p$ scattering cross section vs M_2 as the curve with blue pluses. Starting off at large M_2, we see that as M_2 is decreased the $\sigma^{\rm SI}(\tilde{Z}_1 p)$ cross section increases, and the increase is substantially larger than the case of a binolike LSP. Recall this cross section proceeds mainly via light h exchange which depends on a product of gaugino and Higgsino components of the neutralino LSP [25]. In this case, the wino component, which involves the larger $SU(2)$ gauge coupling g, becomes enhanced leading to the large cross section. For small enough $M_2 < 250$ GeV, the cross section turns around and decreases with decreasing M_2 since the $\tilde{Z}_1$ becomes more purely winolike and the Higgsino components are diminished. We note here that, though the cross section in Fig. 6 exceeds the stated bounds ($1–2 \times 10^{-9}$ pb for $m_{\tilde{Z}_1} = 100–200$ GeV) in Ref. [29], these bounds are not directly applicable because they were obtained assuming the neutralino constitutes the entire dark matter content of the Universe. For the natural SUSY scenario, the rates in direct detection experiments could be much smaller, as these scale by the neutralino fraction of the total local dark matter density. A winolike neutralino that forms the bulk of the local dark matter would be excluded.

In Fig. 7, we show the spin-dependent direct detection cross section $\sigma^{\rm SD}(\tilde{Z}_1 p)$ vs M_2 as the blue curve. Here, the SD scattering cross section which proceeds mainly by Z exchange becomes large since there is less cancellation in the Z – Higgsino – Higgsino coupling. For small enough M_2, then again the cross section turns over and decreases due to the diminishing Higgsino components. We see that the cross section exceeds its 90% C.L. IceCube upper limit $\sim 1.5 \times 10^{-4}$ pb [31] obtained assuming that LSPs in the Sun annihilate dominantly to W pairs if $M_2 < 700$ GeV. As discussed earlier, the expected event rate must be rescaled by ξ ($= 0.01–0.1$ for thermally produced wino LSPs), before comparing with IceCube limits. Then the IceCube limit on the cross section will be correspondingly degraded, assuming that the neutralino density in the Sun is determined by equilibrium between capture and annihilation rates. The RNSw scenario satisfies the IceCube bound assuming that the wino relic density is close to its thermally produced value and that the axion or some other particle makes up the remainder of the dark matter. Models where the dark matter is dominantly a winolike neutralino are strongly excluded by IceCube.

In Fig. 8, we show $\langle \sigma v \rangle|_{v \to 0}$ vs M_2 as the blue shaded curve. In this case, as M_2 falls, then $\tilde{Z}_1\tilde{Z}_1 \to WW$ becomes large, and the annihilation rate increases. One might expect increased likelihood for indirect WIMP detection via gamma rays and antimatter detection. However, the increased annihilation rate is counterbalanced by a likely decreasing local WIMP abundance where the detection rate is proportional to the square of the reduced local

abundance. We see that, although the predicted rate naively exceeds the upper limit from Fermi-LAT in Ref. [51], after the ξ^2 scaling discussed above, exclusion is not possible.

IV. GENERAL RESULTS IN M_1 VS M_2 PLANE

While it is instructive to examine natural SUSY models with reduced GUT scale bino- or wino-mass parameters, there is no compelling reason to believe that one parameter is unified with M_3(GUT) while the other is quite different. In general one may have arbitrary gaugino masses, and in fact both may be reduced leading to a mixed bino-wino-Higgsino LSP. Here, we present some illustrative studies of this more general situation. We can choose $M_1 > 0$ by convention. The signs of M_2 and M_3 as well as μ are then physically relevant. Since our purpose is to give a broad brush idea of how RNS phenomenology of electroweakinos may be altered, we will take M_3 and μ to be fixed at their values for the RNSh benchmark point and display results in the $M_1 - M_2$ plane.[10]

In Fig. 13, we show the M_1 vs M_2 plane for the RNS benchmark model but with M_1 and M_2 as free parameters. The black dot in the upper-right corner denotes the location for unified gaugino masses. The regions of the plot are coded according to the dominant content of the $\tilde{Z}_1$: bino (blue dots), wino (green triangles), and Higgsino (red pluses). The special cases of the previous sections correspond to moving horizontally to the left or vertically down from the unified gaugino mass point. We start the scans at $M_1 = 50$ GeV and scan both signs of M_2. Here, and in subsequent figures, the band with $|M_2| \lesssim 150$ GeV is excluded by the LEP2 bound on the chargino. In the half-plane with $M_2 < 0$, the additional region without any shading corresponds to a charged LSP ($m_{\tilde{W}_1} < m_{\tilde{Z}_1}$) and so is excluded by cosmological considerations.

In Fig. 14, we show the $\tilde{W}_1 - \tilde{Z}_1$ mass gap in the M_1 vs M_2 plane for the RNS benchmark model. The purple shaded region has mass gaps between 10 and 20 GeV and corresponds to the bulk of the Higgsino-like LSP region along with the winolike LSP region. As expected, the mass gap becomes small when $\tilde{W}_1$ and $\tilde{Z}_1$ are both Higgsino-like ($|\mu| \ll |M_{1,2}|$) or when these are both very winolike ($M_2 \ll |\mu|$). It also becomes small along the boundary of the region in the lower half-plane where the chargino becomes the LSP. It is mainly when one moves to small M_1, or large $|M_2|$ and moderate M_1, that this mass gap exceeds 40–50 GeV, so that the daughter leptons from chargino decays are expected to be relatively hard.

The $\tilde{Z}_2 - \tilde{Z}_1$ mass gap is shown in the M_1 vs M_2 plane in Fig. 15. Typically the smallest mass gap occurs when we have a Higgsino-like LSP as in the case of gaugino mass unification in the upper right part of the plane, or in the region where M_1 and $|M_2|$ are both much larger than μ ($M_2 < 0$). A small (purple) mass region also occurs when $M_1 \sim |2M_2|$ (lower half plane) so that the weak scale values of M_1 and $|M_2|$ become comparable upon renormalization group evolution; i.e., the bino and wino become nearly degenerate, but the states remain nearly pure winos and binos because of opposite signs of their mass terms. In this very low $\tilde{Z}_2 - \tilde{Z}_1$ mass gap region, one might expect enhanced bino-wino coannihilation (BWCA) in the early

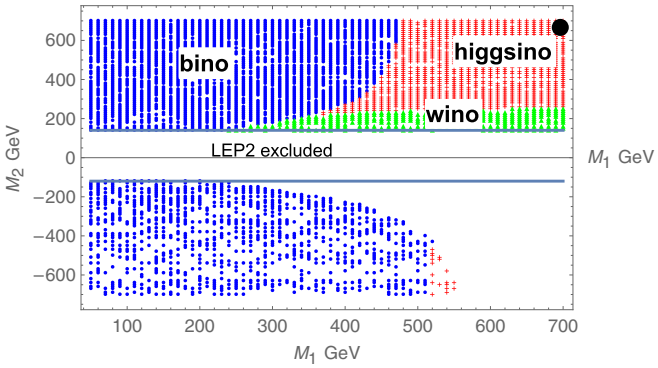

FIG. 13 (color online). Dominant component of the neutralino LSP in the M_1 vs M_2 plane for the RNS SUSY benchmark model. The LSP is dominantly a bino, wino, or Higgsino in the region denoted by blue dots, red pluses, and green crosses, respectively. Other parameters are fixed at their values for the RNSh model point in Table I. In the region marked LEP2 excluded, $m_{\tilde{W}_1} < 100$ GeV, whereas in the remaining unshaded region of the lower half-plane, $m_{\tilde{W}_1} < m_{\tilde{Z}_1}$.

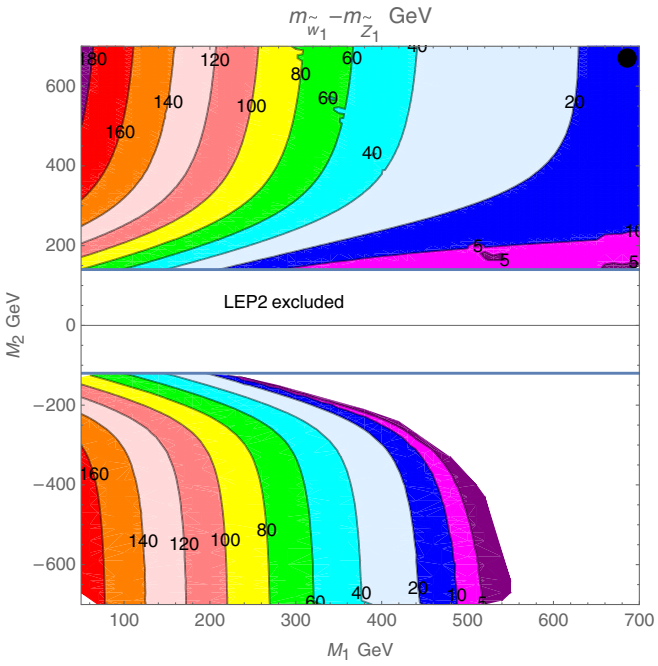

FIG. 14 (color online). The $m_{\tilde{W}_1} - m_{\tilde{Z}_1}$ mass gap in the M_1 vs M_2 plane for the RNS SUSY benchmark model.

[10]The electroweak sector should be almost insensitive to M_3 but will, of course, be sensitive to the sign of μ.

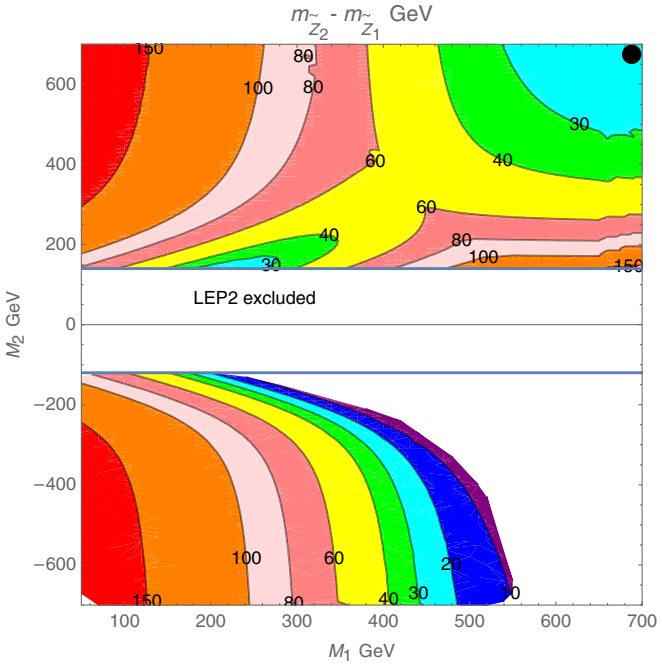

FIG. 15 (color online). The $m_{\tilde{Z}_2} - m_{\tilde{Z}_1}$ mass gap in the M_1 vs M_2 plane for the RNS SUSY benchmark model.

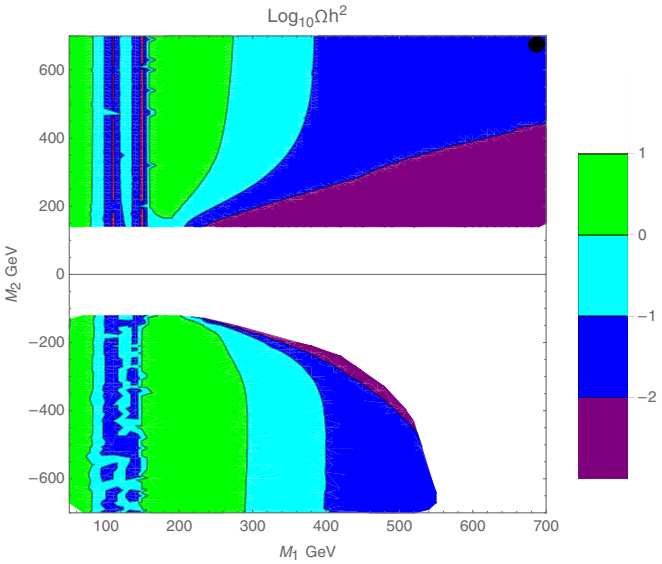

FIG. 16 (color online). Thermally produced neutralino relic abundance in the M_1 vs M_2 plane for the RNS SUSY benchmark model.

Universe [58]. Note that the $\tilde{Z}_2 - \tilde{Z}_1$ mass gap in especially the upper half-plane exceeds 50 GeV for a large swath of the plane and is larger than M_Z and even m_h over a substantial part. This should make for interesting signals at LHC13 via the multilepton, WZ, and Wh plus E_T^{miss} channels at LHC13. It is also noteworthy that a region exists where *both* the $\tilde{W}_1 - \tilde{Z}_1$ and $\tilde{Z}_2 - \tilde{Z}_1$ mass gaps fall below 10 GeV. This occurs in the narrow crescent at large M_1 in the lower half-plane. This region might be challenging even at the ILC if the heavier charginos and neutralinos are kinematically inaccessible. In this case, techniques using initial state photon radiation might be required [59].

We note that, while we have focused on the mass gap between the lighter charginos and neutralinos and the $\tilde{Z}_1$, there is a substantial region of the parameter space of natural SUSY models where signals from the heavier charginos and neutralinos should be accessible at LHC13. Because CMS and ATLAS LHC searches [52,53] tend to employ hard cuts, it is entirely possible that signals from the heavy states (assuming these are within the LHC13 reach) reveal themselves more easily than signals for the lighter states.

The thermally produced neutralino relic density is shown in Fig. 16. The regions with very low relic density $\Omega_{\tilde{Z}_1} h^2 \lesssim 0.01$ are 1) the winolike LSP region along with 2) the BWCA strip in the lower half-plane where $m_{\tilde{W}_1} \simeq m_{\tilde{Z}_1}$ and 3) the resonance annihilation regions where $2m_{\tilde{Z}_1} \sim M_Z$ or m_h (the vertical strips at low M_1). The thermal relic density is also below its observed value in the Higgsino region or in parts of the mixed bino-Higgino LSP region. In these regions, we will need either additional dark matter particles or nonthermal production of neutralinos to match the measured value of cold dark matter relic density. The boundary of the light- and dark-blue shaded region is where we have a well-tempered neutralino of which the thermal neutralino relic density can saturate the cold dark matter. In the light-blue and green-shaded parts of the plane (deep in the bino LSP and away from the Z and h resonances), the relic density of neutralinos must be diluted by entropy production late in the history of the Universe or else the $\tilde{Z}_1$ must be made to decay either via R-parity violating interactions or decay to an alternative LSP (e.g., an axino).

We do not show the dark matter detection cross sections in this plane, partly because for the most part we do not expect that these will unambiguously constrain the parameter regions for reasons that we discussed earlier regarding the assumed local density of WIMPs.

V. CONCLUSIONS

Supersymmetric models with radiatively driven naturalness are especially interesting since they allow for $M_Z, m_h \sim 100$ GeV while sparticles other than Higgsinos can naturally be at the multi-TeV scale. Such spectra seem to be required by reconciling naturalness with LHC8 sparticle search constraints and with the measured value of the Higgs boson mass [60,61]. Most previous analyses have examined RNS models in the context of gaugino mass unification. In that case, the LSP is expected to be Higgsino-like and constitute only a portion of the dark matter while axions could make up the remainder. The light

Higgsinos required by naturalness can evade LHC searches because of their compressed spectrum: Higgsino decays release only small visible energy, so that their production remains hidden under Standard Model backgrounds.

These results follow from requiring both naturalness and gaugino mass unification. We regard naturalness to be one of the main motivations for supersymmetry. In contrast, while gaugino mass unification is highly motivated by the simplest GUT models, it is easy to construct GUTs with nonuniversal gaugino masses at no cost to naturalness. Gaugino mass nonuniversality results if vacuum expectation values of the auxiliary fields that spontaneously break supersymmetry also break the GUT symmetry. The main requirement from LHC searches is that $M_3 \sim m_{\tilde{g}} \gtrsim 1.3$ TeV. The values of bino and wino mass parameters are relatively unconstrained. If their weak scale values are similar to or less than $|\mu|$, then the LSP can be either binolike or winolike (or a mixture) instead of just Higgsino-like at no cost to naturalness. In such a case, both the collider expectations and dark matter/WIMP search expectations change in important ways.

We have shown that, in the case of natural SUSY models with enhanced bino LSP content, increased mass gaps $\tilde{W}_1 - \tilde{Z}_1$ and $\tilde{Z}_2 - \tilde{Z}_1$ are expected on account of bino-Higgsino mixing. The harder decay products of $\tilde{W}_1$ and $\tilde{Z}_2$ lead to discernable effects such as the presence of dilepton mass edges in LHC events, and perhaps additional light electroweakino pair production processes at the ILC involving also $\tilde{Z}_3$ production. In the winolike LSP case, then only the $\tilde{Z}_2 - \tilde{Z}_1$ mass gap opens up, while the $\tilde{W}_1 - \tilde{Z}_1$ gap becomes tighter. This situation should be readily discernable at the ILC, especially with the availability of polarized beams. Of course, if M_2 and $|\mu|$ both assume modest values, the heavier states $\tilde{W}_2$, $\tilde{Z}_{3,4}$ will also be accessible at the LHC, and electroweak chargino and neutralino production will lead to a rich variety of multilepton, WZ and Wh plus $E_T^{\rm miss}$ events that are already being searched for [52,53,56], and possibly also spectacular $W^{\pm}W^{\pm} + E_T^{\rm miss}$ events without additional jet activity. In such a scenario, the ILC would become both a Higgsino and a wino/bino factory, and it should be possible to perform a detailed bottom-up study of the electroweakino sector, assuming that all states are kinematically accessible [62].

Expectations for WIMP searches also change. In the case of a binolike LSP, we generally expect a larger thermal abundance of neutralino dark matter. While it is possible to obtain a well-tempered neutralino that saturates the observed cold dark matter relic density, the thermal neutralino density is often too large, in which case it needs to be diluted by late-time entropy production or else allowed to decay. As a result, the neutralino contribution to the relic density today depends on the (unknown) physics, leading to significant uncertainties in prediction of rates for direct detection searches. While this makes it difficult to use experimental bounds from LUX/XENON100 [29] and other experiments to unambiguously exclude portions of parameter space without a complete model of particle physics and cosmology, these searches could lead to a discovery.

In the case of natural SUSY with a winolike WIMP, then one expects an even lower local abundance from thermally produced neutralinos as compared to the value for Higgsino-like LSPs. The measured relic density must then be made up by other (non-WIMP) relics of which axions may be the most promising, or via WIMP production from late decays of heavy particles. In view of the resulting uncertainty in the expectation for local density of neutralino dark matter, we once again advocate using caution when interpreting the absence of events in direct and indirect dark matter searches to exclude ranges of model parameters.

To sum up, in our view, supersymmetric GUTs remain the most attractive solution to the naturalness problem plaguing the Standard Model, and light Higgsinos are the most robust consequence of naturalness considerations. If electroweak gaugino mass parameters happen to assume modest values—this is not required by naturalness but is completely compatible with it—there could be spectacular signals from electroweak gaugino production at the LHC in multilepton $+ E_T^{\rm miss}$, $WZ + E_T^{\rm miss}$, $Wh + E_T^{\rm miss}$, and $W^{\pm}W^{\pm} + E_T^{\rm miss}$ channels. Direct and indirect searches for WIMPs could also reveal a signal even in the case of a depleted local abundance of WIMPs. If natural supersymmetry is realized with fortuitously low gaugino masses, then prospects for SUSY discovery at LHC13 will be vastly improved since signals from *several* chargino and/or neutralino states might also be observable. Production of light electoweakino states at ILC—as required by naturalness [41]—remains true but with even richer prospects since both gauginos and Higgsinos could be kinematically accessible.

ACKNOWLEDGMENTS

We thank A. Mustafayev for checking several calculations and for pointing out an error in the first version of the text. This work was supported in part by the US Department of Energy, Office of High Energy Physics. H. B. would like to thank the William I. Fine Institute for Theoretical Physics at the University of Minnesota for hospitality while this work was completed.

[1] J. Lykken and M. Spiropulu, Sci. Am. **310N5**, 36 (2014).
[2] H. Baer, V. Barger, P. Huang, D. Mickelson, A. Mustafayev, and X. Tata, Phys. Rev. D **87**, 115028 (2013).
[3] J. R. Ellis, K. Enqvist, D. V. Nanopoulos, and F. Zwirner, Mod. Phys. Lett. A **01**, 57 (1986).
[4] R. Barbieri and G. Giudice, Nucl. Phys. **B306**, 63 (1988).
[5] R. Kitano and Y. Nomura, Phys. Lett. B **631**, 58 (2005); Phys. Rev. D **73**, 095004 (2006).
[6] H. Baer, V. Barger, P. Huang, A. Mustafayev, and X. Tata, Phys. Rev. Lett. **109**, 161802 (2012). For somewhat different viewpoints on the interpretation of $\Delta_{\mathbf{EW}}$ (which have no impact on its use in this paper), see Ref. [7].
[7] L. Girardello and M. T. Grisaru, Nucl. Phys. **B194**, 65 (1982).
[8] K. Chan, U. Chattopadhyay, and P. Nath, Phys. Rev. D **58**, 096004 (1998).
[9] H. Baer, V. Barger, and D. Mickelson, Phys. Rev. D **88**, 095013 (2013); A. Mustafayev and X. Tata, Indian J. Phys. **88**, 991 (2014); H. Baer, V. Barger, D. Mickelson, and M. Padeffke-Kirkland, Phys. Rev. D **89**, 115019 (2014).
[10] S. Martin, Phys. Rev. D **89**, 035011 (2014).
[11] G. Aad *et al.* (ATLAS Collaboration), J. High Energy Phys. 09 (2014) 176.
[12] S. Chatrchyan *et al.* (CMS Collaboration), J. High Energy Phys. 06 (2014) 055.
[13] H. Baer, V. Barger, M. Padeffke-Kirkland, and X. Tata, Phys. Rev. D **89**, 037701 (2014).
[14] H. Baer, V. Barger, P. Huang, D. Mickelson, A. Mustafayev, W. Sreethawong, and X. Tata, J. High Energy Phys. 12 (2013) 013.
[15] C. Han, A. Kobakhidze, N. Liu, A. Saavedra, L. Wu, and J. M. Yang, J. High Energy Phys. 02 (2014) 049.
[16] H. Baer, A. Mustafayev, and X. Tata, Phys. Rev. D **89**, 055007 (2014).
[17] Z. Han, G. D. Kribs, A. Martin, and A. Menon, Phys. Rev. D **89**, 075007 (2014).
[18] H. Baer, A. Mustafayev, and X. Tata, Phys. Rev. D **90**, 115007 (2014).
[19] R. D. Peccei and H. R. Quinn, Phys. Rev. Lett. **38**, 1440 (1977); S. Weinberg, Phys. Rev. Lett. **40**, 223 (1978); F. Wilczek, Phys. Rev. Lett. **40**, 279 (1978).
[20] K.-Y. Choi, J. E. Kim, H. M. Lee, and O. Seto, Phys. Rev. D **77**, 123501 (2008); H. Baer, A. Lessa, S. Rajagopalan, and W. Sreethawong, J. Cosmol. Astropart. Phys. 06 (2011) 031.
[21] J. Ellis, K. Enqvist, D. V. Nanopoulos, and K. Tamvakis, Phys. Lett. B **155**, 381 (1985); M. Drees, Phys. Lett. B **158**, 409 (1985).
[22] G. Anderson, H. Baer, C. h. Chen, and X. Tata, Phys. Rev. D **61**, 095005 (2000).
[23] K. Choi, A. Falkowski, H. P. Nilles, M. Olechowski, and S. Pokorski, J. High Energy Phys. 11 (2004) 076.
[24] I. Gogoladze, F. Nasir, and Q. Shafi, Int. J. Mod. Phys. A **28**, 1350046 (2013).
[25] H. Baer and X. Tata, *Weak Scale Supersymmetry: From Superfields to Scattering Events*, (Cambridge University Press, Cambridge, England, 2006).
[26] H. Baer, C. Balazs, and A. Belyaev, J. High Energy Phys. 03 (2002) 042.
[27] M. Misiak *et al.*, Phys. Rev. Lett. **98**, 022002 (2007).
[28] J. P. Lees *et al.* (*BABAR* Collaboration), Phys. Rev. D **86**, 052012 (2012); T. Saito *et al.* (Belle Collaboration), Phys. Rev. D **91**, 052004 (2015).
[29] D. Akerib *et al.* (LUX Collaboration), Phys. Rev. Lett. **112**, 091303 (2014); see also E. Aprile *et al.* (XENON100 Collaboration), Phys. Rev. Lett. **109**, 181301 (2012), for results from an earlier, independent search.
[30] H. Baer, K. Y. Choi, J. E. Kim, and L. Roszkowski, Phys. Rep. **555**, 1 (2015).
[31] M. Aartsen *et al.* (IceCube Collaboration), Phys. Rev. Lett. **110**, 131302 (2013).
[32] H. Baer, F. Paige, S. Protopopescu, and X. Tata, arXiv:hep-ph/0312045.
[33] H. Baer, V. Barger, P. Huang, D. Mickelson, A. Mustafayev, W. Sreethawong, and X. Tata, Phys. Rev. Lett. **110**, 151801 (2013).
[34] W. Bennakker, R. Hopker, and M. Spira, arXiv:hep-ph/9611232.
[35] A. Chamseddine, P. Nath, and R. Arnowitt, Phys. Lett. B **129**, 445 (1983); D. Dicus, S. Nandi, and X. Tata, Phys. Lett. B **129**, 451 (1983); H. Baer and X. Tata, Phys. Lett. B **155**, 278 (1985); H. Baer, K. Hagiwara, and X. Tata, Phys. Rev. D **35**, 1598 (1987); P. Nath and R. L. Arnowitt, Mod. Phys. Lett. A **02**, 331 (1987); R. Barbieri, F. Caravaglios, M. Frigeni, and M. L. Mangano, Nucl. Phys. **B367**, 28 (1991); H. Baer and X. Tata, Phys. Rev. D **47**, 2739 (1993); H. Baer, C. Kao, and X. Tata, Phys. Rev. D **48**, 5175 (1993); J. L. Lopez, D. V. Nanopoulos, X. Wang, and A. Zichichi, Phys. Rev. D **52**, 142 (1995); V. Barger, C. Kao, and T. Li, Phys. Lett. B **433**, 328 (1998); V. Barger and C. Kao, Phys. Rev. D **60**, 115015 (1999); H. Baer, M. Drees, F. Paige, P. Quintana, and X. Tata, Phys. Rev. D **61**, 095007 (2000); K. Matchev and D. Pierce, Phys. Lett. B **467**, 225 (1999); E. Accomando, R. L. Arnowitt, and B. Dutta, Phys. Lett. B **475**, 176 (2000); S. Dube, J. Glatzer, S. Somalwar, A. Sood, and S. Thomas, J. Phys. G **39**, 085004 (2012).
[36] H. Baer, C. H. Chen, F. Paige, and X. Tata, Phys. Rev. D **50**, 4508 (1994); **53**, 6241 (1996); H. Baer, T. Krupovnickas, S. Profumo, and P. Ullio, J. High Energy Phys. 10 (2005) 020; S. Bhattacharya, A. Datta, and B. Mukhopadhyaya, Phys. Rev. D **78**, 115018 (2008).
[37] H. Baer, V. Barger, S. Kraml, A. Lessa, W. Sreethawong, and X. Tata, J. High Energy Phys. 03 (2012) 092.
[38] T. Han, S. Padhi, and S. Su, Phys. Rev. D **88**, 115010 (2013).
[39] T. A. W. Martin and D. Morrissey, J. High Energy Phys. 12 (2014) 168.
[40] H. Baer, V. Barger, A. Lessa, W. Sreethawong, and X. Tata, Phys. Rev. D **85**, 055022 (2012).
[41] H. Baer, V. Barger, D. Mickelson, A. Mustafayev, and X. Tata, J. High Energy Phys. 06 (2014) 172.
[42] T. Tsukamoto, K. Fujii, H. Murayama, M. Yamaguchi, and Y. Okada, Phys. Rev. D **51**, 3153 (1995).
[43] H. Baer, R. B. Munroe, and X. Tata, Phys. Rev. D **54**, 6735 (1996).
[44] M. Dine, W. Fischler, and M. Srednicki, Phys. Lett. B **104**, 199 (1981); A. P. Zhitnitskii, Sov. J. Appl. Phys. **31**, 260 (1980).
[45] K. J. Bae, H. Baer, and H. Serce, Phys. Rev. D **91**, 015003 (2015).

[46] K. J. Bae, H. Baer, and E. J. Chun, Phys. Rev. D **89**, 031701 (2014).
[47] H. Baer, V. Barger, and D. Mickelson, Phys. Lett. B **726**, 330 (2013).
[48] H. Baer, C. Balazs, A. Belyaev, and J. O'Farrill, J. Cosmol. Astropart. Phys. 09 (2003) 007.
[49] C. Cheung, L. J. Hall, D. Pinner, and J. T. Ruderman, J. High Energy Phys. 05 (2013) 100.
[50] P. Huang and C. E. M. Wagner, Phys. Rev. D **90**, 015018 (2014).
[51] M. Ackermann *et al.*, Phys. Rev. D **89**, 042001 (2014).
[52] V. Khatchatryan *et al.* (CMS Collaboration), Eur. Phys. J. C **74**, 3036 (2014).
[53] G. Aad *et al.* (ATLAS Collaboration), J. High Energy Phys. 05 (2014) 071.
[54] T. Gherghetta, G. F. Giudice, and J. D. Wells, Nucl. Phys. **B559**, 27 (1999).
[55] A. G. Delannoy *et al.*, Phys. Rev. Lett. **111**, 061801 (2013).
[56] ATLAS Collaboration, Report No. ATLAS-CONF-2014-062.
[57] T. Moroi and L. Randall, Nucl. Phys. **B570**, 455 (2000); B. S. Acharya, G. Kane, S. Watson, and P. Kumar, Phys. Rev. D **80**, 083529 (2009); R. Allahverdi, B. Dutta, and K. Sinha, Phys. Rev. D **87**, 075024 (2013).
[58] H. Baer, T. Krupovnickas, A. Mustafayev, E. K. Park, S. Profumo, and X. Tata, J. High Energy Phys. 12 (2005) 011.
[59] M. Berggren, F. Brmmer, J. List, G. Moortgat-Pick, T. Robens, K. Rolbiecki, and H. Sert, Eur. Phys. J. C **73**, 2660 (2013).
[60] G. Aad *et al.* (ATLAS Collaboration), Phys. Lett. B **716**, 1 (2012).
[61] S. Chatrchyan *et al.* (CMS Collaboration), Phys. Lett. B **716**, 30 (2012).
[62] S. Y. Choi, A. Djouadi, M. Guchait, J. Kalinowski, H. S. Song, and P. M. Zerwas, Eur. Phys. J. C **14**, 535 (2000); **22**, 563 (2001).